Vertically Aligned Sulfur-Doped ZnO Nanowires Synthesized via Chemical Vapor Deposition

Seung Yong Bae, Hee Won Seo, and Jeunghee Park*

Department of Chemistry, Korea University, Jochiwon 339-700, South Korea

Received: September 12, 2003; In Final Form: February 25, 2004

High-density ZnO nanowires doped with 4 atom % sulfur (S) and pure ZnO nanowires were grown vertically aligned on a silicon substrate. They were synthesized via chemical vapor deposition of a Zn or Zn/S powder mixture at 500 °C. The S-doped ZnO nanowires usually form bundles. The average diameter of the S-doped ZnO nanowires and ZnO nanowires is 20 and 50 nm, respectively. They consist of single-crystalline wurtzite ZnO crystals with a uniform growth direction of [001]. Elemental mapping reveals that the S doping takes place mainly at the surface of the nanowires with a thickness of a few nanometers. X-ray diffraction data suggest that the incorporation of S would expand the lattice constants of ZnO. The photoluminescence and cathodoluminescence of S-doped ZnO nanowires exhibit a significantly enhanced green emission band that comes from the S-doped surface region of the nanowires.

1. Introduction

Zinc oxide (ZnO) is one of the most promising materials for the fabrication of optoelectronic devices operating in the blue and UV region and for gas sensing applications,[1,2] owing to a direct wide band gap ($E_g = 3.37$ eV at room temperature) and large exciton binding energy (60 meV). Stimulated by the novel properties of carbon nanotubes, quasi-one-dimensional nanostructures of ZnO are currently the subject of intensive research because of the potential for nanoscale electronic and optoelectronic applications.[3−9] Recently, doping of the nanostructures has become an important issue for the more diverse range of applications.[10−13] S-doping in a ZnO system is expected to modify the electrical and optical properties because of the large electronegativity and size differences between S and O. In addition, E_g engineering might be possible because of the larger E_g of ZnS (3.66 eV) compared to that of ZnO. Regardless of these possibilities, S has been rarely doped in ZnO because of problems in fabrication owing to the significant difference between S stabilization and growth temperature. Recently, Geng et al. reported the synthesis of S-doped ZnO nanowires by a physical evaporation of ZnS powders.[14] They showed a blue shift of photoluminescence due to the S doping. However, the structure- and composition-controlled synthesis of S-doped ZnO nanowires is still a challenging research topic.

Here we present a synthesis of a vertically aligned S-doped ZnO nanowire array via chemical vapor deposition (CVD) of Zn and S powders at a low temperature, 500 °C. In order to elucidate the effect of S doping on the physical properties of ZnO nanowires, we also synthesized vertically aligned ZnO nanowires using a CVD of Zn at 500 °C. These ZnO nanowires grown on silicon (Si) substrates were exclusively used for the growth of the S-doped ZnO nanowires. The structural and optical properties of the nanowires were thoroughly investigated using scanning electron microscopy (SEM), transmission electron microscopy (TEM), electron energy loss spectroscopy (EELS), X-ray diffraction (XRD), X-ray photoelectron spectroscopy (XPS), Raman spectroscopy, photoluminescence (PL), and cathodoluminescence (CL).

2. Experimental Section

Synthesis of the nanowires was carried out in a tube furnace. For the preparation of the ZnO nanowires, the Si substrates were coated with $HAuCl_4 \cdot 3H_2O$ (98+%, Sigma) in ethanol solution, forming the Au catalytic nanoparticles. Zn (99.998%, Aldrich) powders were placed in a quartz boat located inside a quartz tube reactor. The substrate was positioned on the quartz boat containing the Zn powders. The temperature of the reactor was maintained as 500 °C for 2 h. Argon (Ar) was flowed at a rate of 500 sccm. A blue-tinted white-colored film deposited on the whole substrate. For the synthesis of S-doped ZnO nanowires, the S (99.999%, Aldrich) powders were located at the entrance of the quartz tube and the Si substrate deposited with the pregrown ZnO nanowires was placed on the boat containing the Zn powders. The flow rate of Ar, the temperature, and the growth time were maintained as 500 sccm, 500 °C, and 2 h, respectively. White-colored filmlike product was newly formed on the whole substrate. The as-grown materials were characterized and analyzed by SEM (Hitachi S-4300), TEM (JEOL JEM-2010, 200 kV), electron diffraction (ED), energy-dispersive X-ray spectroscopy (EDX), EELS (GATAN GIF-2000) attached to TEM (Philips CM200), XPS (PHI 5800), and powder XRD (Philips X'PERT MPD). PL measurements were conducted at 8 and 300 K (room temperature), with the 325 nm line of a helium−cadmium (He−Cd) laser. The laser power was about 1 kW/cm^2. The room temperature CL (Gatan MonoCL2) measurement was performed at an acceleration voltage of 10 kV.

3. Results and Discussion

Figure 1a shows the SEM image for the wirelike nanostructures homogeneously grown on a large area of the Si substrate. They are vertically aligned on the substrate. The length is about 10 μm. Further analyses described below reveal that these nanowires are indeed composed of S-doped ZnO crystals. Figure

* Corresponding author. E-mail: parkjh@korea.ac.kr.

10.1021/jp036720k CCC: $27.50
Published on Web 04/02/2004

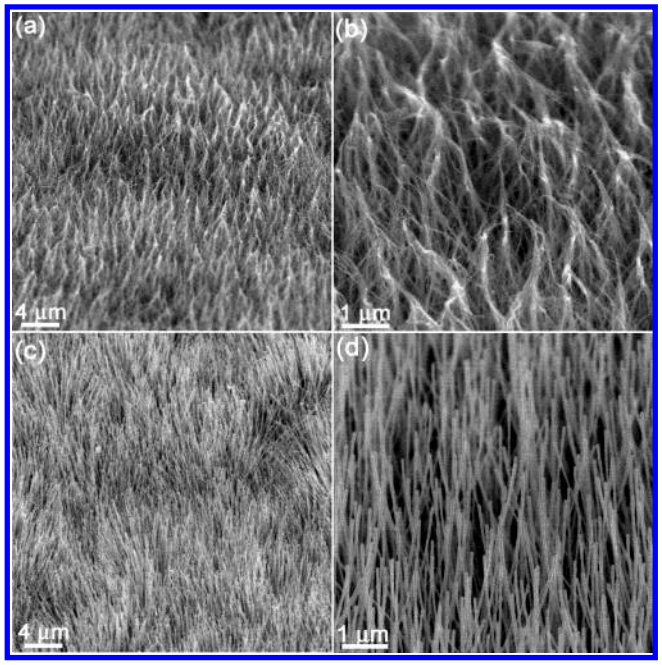

Figure 1. (a) SEM micrograph shows the vertically aligned S-doped ZnO nanowires on a large area of the Si substrate. (b) The magnified view shows that the nanowires form the bundles. (c) The ZnO nanowires are homogeneously grown with high density and (d) vertically aligned on the Si substrate.

1b shows that most of the nanowires form aligned bundles. A further magnified view reveals that a bundle consists of 10−100 nanowires. Parts c and d of Figure 1 show SEM images for the pure ZnO nanowires. The vertically aligned ZnO nanowires are grown homogeneously over a large area of the substrate. The length is also about 10 μm. The surface of the ZnO nanowires is clean without any nanoparticle impurity.

A TEM image representing the general morphology of the S-doped ZnO nanowires is displayed in Figure 2a. It reveals that the nanowires are straight, and their diameter is uniformly 20 nm. Figure 2b shows the high-resolution TEM (HRTEM) image for the nanowire having a diameter of 8 nm. No amorphous phase or outer layers exist. The selected-area ED (SAED) pattern shows that the nanowire consists of single-crystalline ZnO crystals with the [001] direction parallel to the long axis (inset). Figure 2c shows the atomic-resolved image for a selected area of the nanowire. The (002) fringes perpendicular to the growth direction are separated by 2.6 Å, which is consistent with that of the bulk wurtzite ZnO crystal (a = 3.249 82Å, c = 5.206 61Å; JCPDS Card No. 36-1451). No stacking faults are found in the lattice planes. All nanowires have the [001] growth direction. EDX identifies that the composition of the nanowires is Zn, O, and S (Figure 2d). The S content is about 4 atom %. The Cu peak comes from the TEM grid.

Figure 2e shows the TEM image representing the general morphology of the ZnO nanowires. The average diameter of the nanowires is 50 nm. Figure 2f corresponds to an atomic-resolved image of the ZnO nanowire. It reveals that the nanowire is single crystalline and the (001) fringes are separated by 5.2 Å corresponding to that of the bulk wurtzite ZnO crystal. No stacking faults exist in the lattice planes. The SAED confirms that the growth direction of the nanowires is also [001] (inset). All nanowires we observed have the [001] growth direction.

Figure 3 displays the EELS (or energy-filtered TEM) imaging of a S-doped ZnO nanowire. The corresponding TEM image is shown in Figure 3a. The Zn and O elemental mapping was

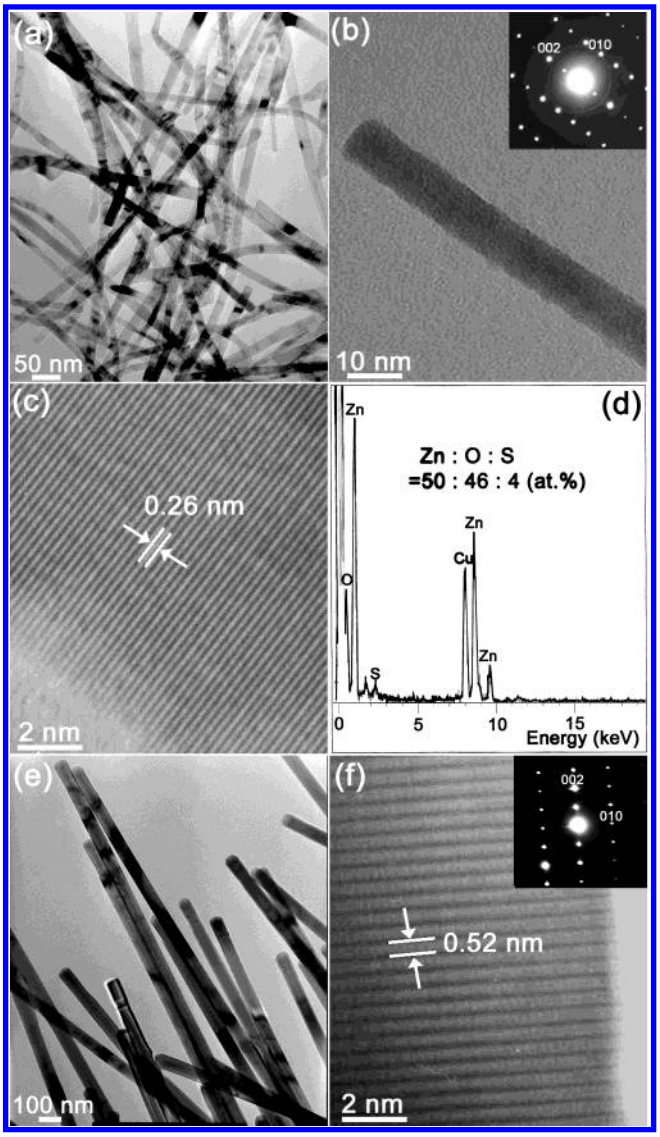

Figure 2. (a) TEM image showing the general morphology of the S-doped ZnO nanowires. The average diameter is 20 nm. (b) HRTEM image for 8 nm diameter ZnO nanowire. The SAED pattern reveals the [001] growth direction (inset). (c) Atomic-resolved image shows that the distance between neighboring (002) planes is about 2.6 Å. (d) EDX data shows 4 atom % S. (e) TEM image reveals a general morphology of the ZnO nanowires. The diameter is uniformly 50 nm. (f) HRTEM image for the ZnO nanowire, showing the (001) fringes perpendicular to the growth direction. The SAED pattern confirms the [001] growth direction

obtained using the energy loss of the L-shell edges ($L_{2,3}$) of Zn (ΔE = 1020 eV) and K-shell edges of O (ΔE = 532 eV), respectively (parts b and c of Figure 3). The brighter points represent a higher concentration of the element, confirming that the core consists of Zn and O elements. Figure 3d shows the S elemental mapping using the energy loss of the L-shell edges ($L_{2,3}$) of S (ΔE = 165 eV). It reveals that the S doping occurs mainly at the surface of the nanowires with a thickness of a few nanometers.

XPS was also used to determine the composition of the S-doped ZnO nanowires. Figure 4a shows the whole scanning spectrum. The peaks located at 1022, 530, and 164 eV corresponds to the electronic states of Zn 2p, O 1s, and S 2p, respectively. The fine XPS spectra of Zn $2p_{3/2}$ and O 1s are also displayed in parts b and c of Figure 4, respectively. Figure 4d shows two overlapped S 2p peaks, corresponding to $2p_{3/2}$

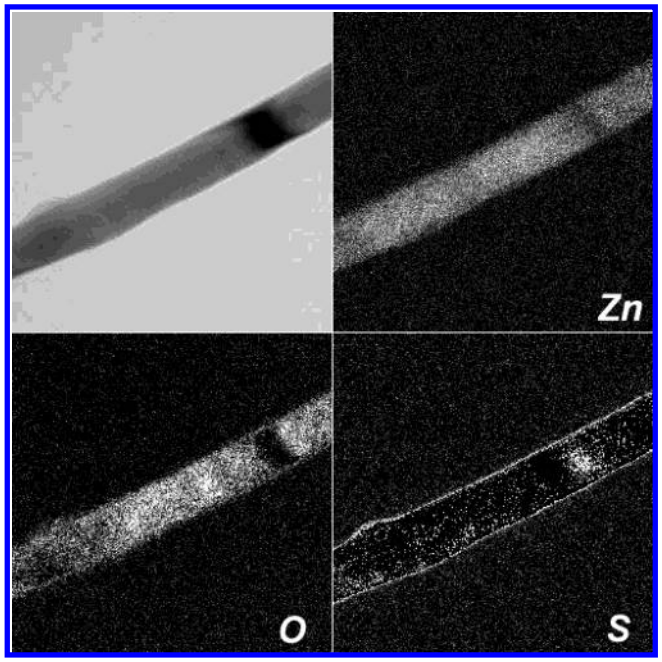

Figure 3. Elemental maps of Zn, O, and S obtained by EELS imaging using inelastic electrons corresponding to the energy loss of each element.

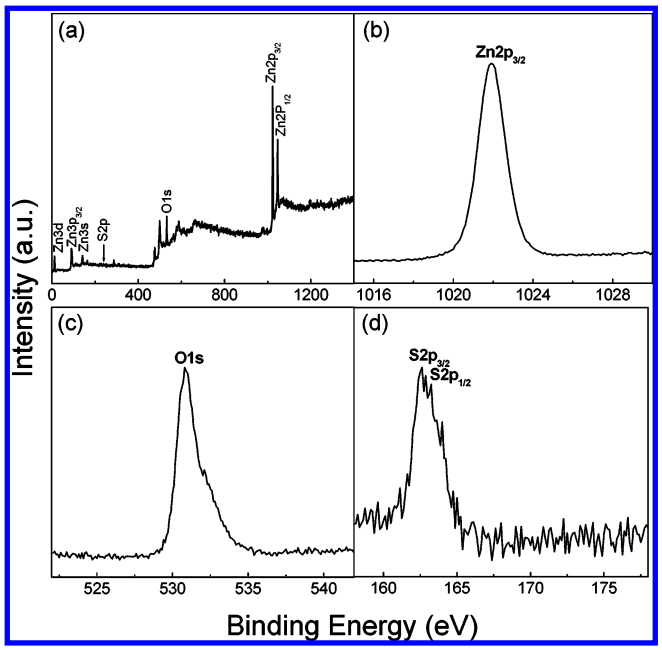

Figure 4. (a) XPS whole scanning spectrum (a) and the fine spectra of Zn $2p_{3/2}$ (b), O 1s (c), and S $2p_{3/2}$ and S $2p_{1/2}$ (d).

and $2p_{1/2}$. The S content is estimated to be about 4 atom % from several measurements.

The growth of the ZnO nanowires on the Au nanoparticles-deposited Si substrate would follow a typical vapor−liquid−solid growth mechanism, although the Au nanoparticles were not detected through the TEM analysis. The size of the nanoparticles would play an important role in determining the diameter of the ZnO nanowires. We utilized these ZnO nanowires for the growth of S-doped ZnO nanowires. The diameter and composition of the S-doped ZnO nanowires is uniform along the wire axis, suggesting that the pregrown ZnO nanowires would be removed and/or reconstructed during the growth of S-doped ZnO nanowires. The smaller diameter of the S-doped ZnO nanowires compared to that of the ZnO nanowires implies that the S-doped ZnO nanowires may start

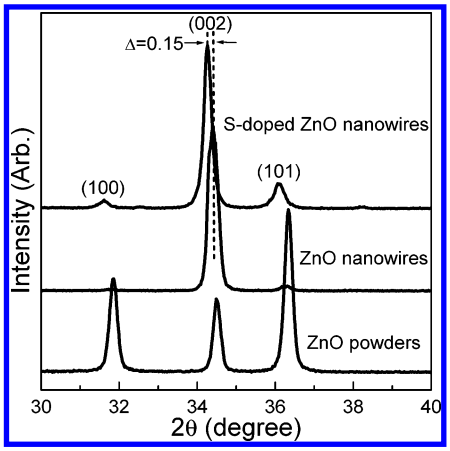

Figure 5. XRD pattern taken from the ZnO powders, ZnO nanowires, and S-doped ZnO nanowires, showing the (100), (002), and (101) peaks of wurtzite ZnO.

growing on the ZnO nanowires. Therefore, we can conjecture the growth process of the present S-doped ZnO nanowires as follows. The Zn, S, and O vapors deposit and form a liquid alloy on the nanosize surface of pregrown ZnO nanowires. The ZnO nanowires can melt into the alloy nanoparticles, providing the Zn and O sources. Following saturation, the S-doped ZnO nanowires precipitate via a vapor−liquid−solid growth mechanism. The vertical alignment and the diameter of the ZnO nanowires would confine the alignment and the diameter of the growing S-doped ZnO nanowires.

The XRD pattern of the S-doped ZnO nanowires in the range of $2\theta = 30-40$ degrees is displayed in Figure 5, along with those of the ZnO nanowires and commercial ZnO powders (99.998%, Aldrich). Three peaks are indexed to (100), (002), and (101) of wurtzite-structured ZnO. No other crystalline forms are detected. The ZnO nanowires show only the (002) peak because of their nearly perfect vertical alignment on the substrate. The S-doped ZnO nanowires are vertically aligned but not as much as the ZnO nanowires. The thinner S-doped ZnO nanowires would have more flexibility than the ZnO nanowires. Therefore, they exhibit weak (100) and (101) peaks.

Careful examination detects a lower angle shift of the S-doped ZnO nanowires relative to that of the ZnO nanowires and powders. The shift of the (002) peaks to lower angle from that of the ZnO nanowires is $\Delta(2\theta) = 0.15°$. This implies an increase in the lattice constant c of the ZnO crystal by 0.4%. The increase of the lattice constants was also observed in the S-doped ZnO film produced by pulsed laser deposition.[15] Most of the S would be incorporated at the interstitial as well as the O sites, leading to an increase of both the lattice constants and the cell volume. This incorporation of S would occur mainly in the surface region of the ZnO nanowires. The peak width is slightly broader than that of the ZnO nanowires, which is probably related with the lattice distortion due to the S substitution.

Figure 6a displays the PL spectrum of the S-doped ZnO nanowires measured at room temperature. We compared it with that of the ZnO nanowires. The excitation energy is 3.815 eV. Both the ZnO and S-doped ZnO nanowires exhibit a peak at 3.27 eV corresponding to the near band edge (NBE) peak that is responsible for the recombination of the free excitons of ZnO.[16] The green emission band around 2.5 eV originates from the recombination of the holes with the electrons occupying the singly ionized O vacancy.[17] The relative intensity of the green emission band to the NBE peak becomes significant for the S-doped ZnO nanowires, which is consistent with the result of Geng et al.[14] The PL spectra measured at 8 K are displayed

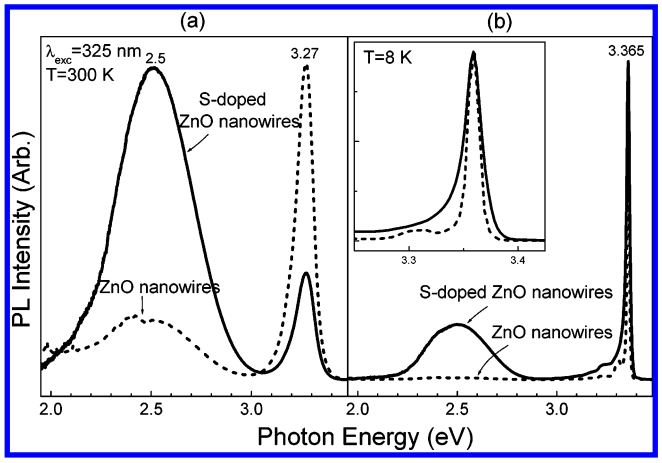

Figure 6. PL spectrum of ZnO nanowires and S-doped ZnO nanowires, measured at (a) room temperature and (b) 8 K. The excitation wavelength is the 325 nm line of a He−Cd laser.

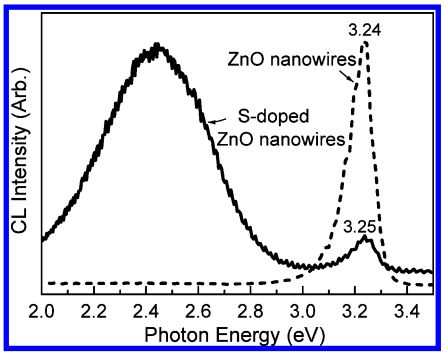

Figure 7. Room temperature CL spectrum of ZnO nanowires and S-doped ZnO nanowires.

in Figure 6b. The NBE peak appears at 3.365 eV (at 300 K) for both the ZnO and S-doped ZnO nanowires. Park et al. attributed the peak at 3.365 eV to the neutral donor bound exciton peak.[18] The bandwidth is larger by a factor of 1.5 for the S-doped ZnO nanowires compared to the ZnO nanowires as shown in the inset. The broader NBE emission band appears at the lower energy region, but there is no noticeable shift to the higher energy region.

Since the S doping occurs mainly at the surface of the ZnO nanowires, the emission comes from the S-doped sites at the surface as well as the undoped or less doped ZnO crystal inside. The inside ZnO part would exhibit the NBE emission at the same photon energy as that of the ZnO nanowires, which largely contribute to the NBE peak intensity. The absorption spectrum of S-doped ZnO film showed that as S is incorporated, the E_g shifts to lower energy.[15] This result was explained by an E_g bowing that probably originates from the formation of localized band edge states due to charge exchange and structural relaxation, proportional to the orbital energy and the size difference of the elements, respectively. The broader NBE emission band at the lower energy region (observed at 8 K) may be related with the E_g decrease that occurred at the S-doped surface region. When S enters the ZnO crystal lattice, it inevitably introduces a lattice distortion. This will give rise to new defects such as oxygen vacancies, which results in the great enhancement of the green emission band.

The CL spectrum of the S-doped ZnO nanowires and the ZnO nanowires was measured at room temperature, showing the NBE peak at a similar position, 3.24 and 3.25 eV, respectively (Figure 7). As the S doping occurs, the intensity of the green emission band is significantly enhanced, which is consistent with the PL result. Therefore, we conclude that the S doping increases the green emission by introducing defects in the ZnO lattice.

4. Conclusions

We report the synthesis of high-density arrays of vertically aligned S-doped ZnO nanowires and ZnO nanowires. As a first step, pure ZnO nanowires were synthesized on Au nanoparticles-deposited Si substrates via CVD of Zn at 500 °C. The average diameter of the ZnO nanowires is 50 nm, and the length is about 10 μm. The S-doped ZnO nanowires were synthesized using the CVD of Zn and S powders. The use of the substrate deposited with the vertically aligned ZnO nanowires results in the successful growth of vertically aligned S-doped ZnO nanowires. The average diameter of the S-doped ZnO nanowires is 20 nm, and the length is about 10 μm. The HRTEM images and SAED patterns confirm that the ZnO nanowires and the S-doped ZnO nanowires consist of single-crystalline wurtzite ZnO crystals grown with the [001] direction.

EDX and XPS reveal that the ZnO nanowires are doped with 4 atom % S. Elemental mapping of EELS reveals that the S doping takes place mainly at the surface of the nanowires with a thickness of a few nanometers. The lower angle shift of the XRD was observed for the S-doped ZnO nanowires, indicating that the S doping would expand the lattice constants of the ZnO. The PL and CL of the S-doped ZnO nanowires show a NBE band at 3.24−3.27 eV (room temperature) and a significantly enhanced green emission compared to that of the ZnO nanowires. The NBE emission of the undoped or less doped inside part would contribute significantly, so the peak appears at the same energy as that of the ZnO nanowires. The strong green emission band is probably due to defects such as oxygen deficiencies at the S doping sites in the surface region of the nanowires.

Acknowledgment. This work was supported by the Korea Science and Engineering Foundation (Project No. R14-2003-033-01003-0) and Korea Research Foundation (Project No. 2003-015-C00265). SEM and XRD analyses were performed at the Korea Basic Science Institute in Seoul.

References and Notes

(1) Cao, H.; Xu, J. Y.; Zhang, D. Z.; Chang, S.-H.; Ho, S. T.; Seelig, E. W.; Liu, X.; Chang, R. P. H. *Phys. Rev. Lett.* **2000**, *84*, 5584.

(2) Dong, L. F.; Cui, Z. L.; Zhang, Z. K. *Nanostruct. Mater.* **1997**, *8*, 815.

(3) Huang, M. H.; Mao, S.; Feick, H.; Yan, H.; Wu, Y.; Kind, H.; Weber, E.; Russo, R.; Yang, P. *Science* **2001**, *292*, 1897.

(4) Pan, Z. W.; Dai, Z. R.; Wang, Z. L. *Science* **2001**, *291*, 1947.

(5) Wu, J.-J.; Liu, S.-C.; Wu, C.-T.; Chen, K.-H.; Chen, L.-C. *Appl. Phys. Lett.* **2002**, *81*, 1312.

(6) (a) Park, W. I.; Kim, D. H.; Jung, S.-W.; Yi, G.-C. *Appl. Phys. Lett.* **2002**, *80*, 4232. (b) Park, W. I.; Yi, G.-C.; Kim, M.; Pennycook, S. J. *Adv. Mater.* **2002**, *14*, 1841.

(7) Goldberger, J.; He, R.; Zhang, Y.; Lee, S.; Yan, H.; Choi, H.-J.; Yang, P. *Nature* **2003**, *422*, 599.

(8) Hu, J. Q.; Li, Q.; Meng, X. M.; Lee, C. S.; Lee, S. T. *Chem. Mater.* **2003**, *15*, 305.

(9) Lao, J. Y.; Huang, J. Y.; Wang, D. Z.; Ren, Z. F. *Nano Lett.* **2003**, *3*, 235.

(10) Cui, Y.; Duan, X.; Hu, J.; Lieber, C. M. *J. Phys. Chem. B* **2000**, *104*, 5213.

(11) Duan, X.; Huang, Y.; Cui, Y.; Wang, J.; Lieber, C. M. *Nature* **2001**, *409*, 66.

(12) Tang, Y. H.; Sham, T. K.; Jürgensen, A.; Hu, Y. F.; Lee, C. S.; Lee, S. T. *Appl. Phys. Lett.* **2002**, *80*, 3709.

(13) Seo, H. W.; Bae, S. Y.; Park, J.; Yang, H.; Kang, M.; Kim, S.; Park, J. C.; Lee, S. Y. *Appl. Phys. Lett.* **2003**, *82*, 3752.

(14) Geng, B. Y.; Wang, G. Z.; Jiang, Z.; Xie, T.; Sun, S. H.; Meng, G. W.; Zhang, L. D. *Appl. Phys. Lett.* **2003**, *82*, 4791.

(15) Yoo, Y.-Z.; Jin, Z.-W.; Chikyow, T.; Fukumura, T.; Kawasaki, M.; Koinuma, H. *Appl. Phys. Lett.* **2002**, *81*, 3798.
(16) Kong, Y. C.; Yu, D. P.; Zhang, B.; Fang, W.; Feng, S. Q. *Appl. Phys. Lett*. **2001**, *78*, 407.
(17) Vanheusden, K.; Warren, W. L.; Seager, C. H.; Tallant, D. R.; Voigt, J. A.; Gnade, B. E. *J. Appl. Phys*. **1996**, *79*, 7983.
(18) Park, W. I.; Jun, Y. H.; Jung, S. W.; Yi, G.-C. *Appl. Phys. Lett.* **2003**, *82*, 964.